# A MATHEMATICAL MODEL OF THE UNIFORMLY FLUIDIZED BED

Ján BEŇA and Ivan HAVALDA

*Department of Chemical Engineering,*
*Institute of Chemical Technology, 880 37 Bratislava*

Received March 10th, 1977

In earlier published papers we have determined admissible geometrical structures (structures of type termed A and B) of equal-diameter spheres providing for the balance of forces — gravity, buoyancy and the force of resistance — on every particle in an unconfined bed. At constant superficial velocity of the fluid, porosity of bed as well as constant physical characteristics of particles and the fluid the bed may be stable for a unique geometrical configuration of the particles only, identical with that of the uniformly fluidized bed. This configuration can be determined for small numbers of the Archimedes group by formulation and solution of a mathematical model provided that the values of Ar, Re and $\varepsilon$ for the uniformly fluidized bed are known.

According to the theoretical model[1,2] the hydrodynamics of the uniformly fluidized bed of equal-diameter spheres at $Ar \leqq 7{\cdot}2$ reduces to the problem of the flow past a particle for in-advance-known boundary conditions. This approach has been applied before[3-5] but a comprehensive formulation of the problem was still missing. The earlier papers[1,2] remove this drawback.

Let the superficial velocity of the fluid, $w$, characterizes a given uniformly fluidized bed, *i.e.* we have $w \in \langle w_{min}, v_t \rangle$, where $w_{min}$ is the velocity at incipient fluidization and $v_t$ is the terminal settling velocity of an individual particle as that in the bed in question in an unconfined fluid of identical properties. To solve the hydrodynamics of the uniformly fluidized bed at the velocity $w$ in the most general case poses *a*) to find all plausible geometrical configurations of particles in the bed providing simultaneously for a balance of the gravity, buoyancy and the friction forces on all particles, *b*) choose from all beds satisfying conditions *a*) the one minimizing the mean specific potential energy of particles forming the bed, or the height of the bed, because only such configuration is that of the uniformly fluidized bed.

Solution of this problem presumes that for an arbitrary particle configuration one is able to determine the resistance force for any particle. Unfortunatelly, this is not the case. In view of the complexity of the problem it is reasonable to combine theory with an experiment avoiding assumptions of dubious validity. For instance, a significant progress would be made by direct experimental determination of the geometrical configuration of particles in uniformly fluidized beds of various porosities. Experimental methods of this type though have been lacking.

In this paper we have used experimental data of Ar, Re, $\varepsilon$ for expansion of the uniformly fluidized bed. For this purpose also a mathematical model has been formulated.

*Some Equations of the Mathematical Model*

From the previous studies[1,2], a uniformly fluidized bed of spherical particles at Ar $\leqq$ 7·2 must exhibit the structures of either the type A or B. Hence only the configuration A and B shall be considered.

If the origin of cylindrical coordinates is put into the center of the particle, as in Fig. 1, then for the corresponding part of the velocity field on the main plane within the boundary flow pattern of surface area $S_1$ equation (*1*) is valid

$$wS_1 = uA + 2\pi \int_{d/2}^{R} v_z(r, \theta, 0)\, r\, \mathrm{d}r\,, \tag{1}$$

where

$$S_1 = H_1 R^2\,, \quad A = H_2 R^2\,, \quad R = \mathrm{d}\sigma(\varepsilon)\left[\varphi(\varepsilon)\right]^{-1/3}\,, \tag{2}$$

$$h/R = \varphi(\varepsilon)\,, \tag{3}$$

$$u = v_z(R, \theta, 0)\,. \tag{4}$$

In these equations each of the presumed structures A or B has its own coefficients $H_1$, $H_2$ and functions $\sigma(\varepsilon)$. These can be found in Table I of ref.[2]. For instance, for the

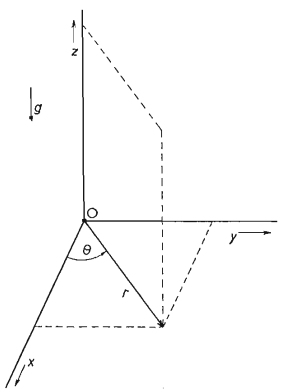


FIG. 1

Orientation of the Cartesian $(x, y, z)$ and Cylindrical $(r, \theta, z)$ Coordinates with the Origin in Particle Center

types $A_1$ and $B_1$, $H_1$ equals 4 while $H_2 = 4 - \pi$ and, after some arrangement of the expression on the last line of that table, we obtain $\sigma(\varepsilon) = \{\pi/[24(1 - \varepsilon)]\}^{1/3}$. For the unknown we shall take the radius $R$ of the boundary circle, the distance, $h$, of adjacent main planes, the value of the function $\varphi(\varepsilon)$ and the distribution of the velocity $v_z(r, \theta, 0)$ on the main plane delimited by the boundary circle for $r \in (r_0, R)$. The superficial velocity of the fluid, $w$, the particle diameter, $d$, and the porosity, $\varepsilon$, (as well as the values of Ar, Re, $\varepsilon$) for the expansion of the uniformly fluidized bed can be assessed experimentally. The unknowns $R$, $h$, $u$ are given by Eqs (2)–(4). Eq. (1) is regarded as given for the purpose of calculation of $\varphi(\varepsilon)$. In addition one needs an equation for the calculation of $v_z(r, \theta, 0)$ which shall be formulated by the following reasoning.

In region delimited on the main plane by the boundary circle, the components of the velocity vector $v_r$, $v_\theta$, $v_z$ satisfy[2] the following conditions:

$$v(r, \theta, 0) = v_z(r, \theta, 0), \quad \text{resp.} \quad v_r(r, \theta, 0) = v_\theta(r, \theta, 0) = 0, \tag{5}$$

when $r \in \langle r_0, R \rangle$,

$$\frac{\partial^2 v_r}{\partial z^2} = 0, \quad \text{or} \quad v_z \frac{\partial v_\theta}{\partial z} = \nu \frac{\partial^2 v_\theta}{\partial z^2}, \quad \text{when} \quad r \in \langle r, R \rangle, \quad z = 0, \tag{6}$$

$$\frac{\partial^2 v_z}{\partial z^2} \neq 0, \quad \text{when} \quad r \in \langle r, R \rangle, \quad z = 0. \tag{7}$$

TABLE I

Values of $\varphi_*^{(1)}(\varepsilon)$ Computed from Eqs (102) and (89); Values $\varphi_*^{(2)}(\varepsilon)$ Computed from (102), (90); $\varphi^{(2)}(\varepsilon) = h/R$ Computed for the Structural Types $B_2$ and $B_3$ Assuming the Fluidized State to Decay on Contact of Particles from Adjacent Main Planes while Articles within the Main Plane do not Contact (Table III in ref.[2])

| $\varepsilon$ | $\varphi_*^{(1)}(\varepsilon)$ | $\varphi_*^{(2)}(\varepsilon)$ | $\varphi^{(2)}(\varepsilon)$ | $\varepsilon$ | $\varphi_*^{(1)}(\varepsilon)$ | $\varphi_*^{(2)}(\varepsilon)$ |
|---|---|---|---|---|---|---|
| 0·400 | 1·0990 | 1·1983 | 1·2638 | 0·450 | 1·0554 | 1·1481 |
| 0·408 | 1·0925 | 1·1906 | 1·2367 | 0·500 | 1·0062 | 1·0934 |
| 0·412 | 1·0891 | 1·1867 | 1·2227 | 0·550 | 0·9532 | 1·0356 |
| 0·416 | 1·0858 | 1·1828 | 1·2083 | 0·600 | 0·8978 | 0·9760 |
| 0·420 | 1·0823 | 1·1789 | 1·1935 | 0·650 | 0·8414 | 0·9158 |
| | | | | 0·700 | 0·7850 | 0·8560 |

From Eqs (5) we obtain

$$\left.\frac{\partial v_r}{\partial \theta}\right|_{\substack{z=0\\ r\in X}} = \left.\frac{\partial^2 v_r}{\partial \theta^2}\right|_{\substack{z=0\\ r\in X}} = \left.\frac{\partial v_r}{\partial r}\right|_{\substack{z=0\\ r\in X}} = \left.\frac{\partial^2 v_r}{\partial r^2}\right|_{\substack{z=0\\ r\in X}} = \left.\frac{\partial v_\theta}{\partial \theta}\right|_{\substack{z=0\\ r\in X}} = \left.\frac{\partial^2 v_\theta}{\partial \theta^2}\right|_{\substack{z=0\\ r\in X}} =$$

$$= \left.\frac{\partial v_\theta}{\partial r}\right|_{\substack{z=0\\ r\in X}} = \left.\frac{\partial^2 v}{\partial r^2}\right|_{\substack{z=0\\ r\in X}} = 0\,, \tag{8}$$

where $X \equiv \langle r_0, R\rangle$.

After substitution from Eqs (5) and (8) into the continuity equation we have

$$\left.\frac{\partial v_z}{\partial z}\right|_{\substack{z=0\\ r\in X}} = 0\,. \tag{9}$$

*The Navier–Stokes equation for the coordinate r.* Because in the gravity field the component of the volume force parallel to the direction of $r$ vanishes and for $z = 0$ Eqs (5), $(6)_1$, (8), (9) are valid, the Navier–Stokes equation for the coordinate $r$ at a steady flow takes the form

$$\left.\frac{\partial p}{\partial r}\right|_{\substack{z=0\\ r\in X}} = 0\,. \tag{10}$$

*The Navier–Stokes equation for the coordinate θ.* From Eqs (5), (6) and (8) there follows that the Navier–Stokes equation for the coordinate $\theta$ reads

$$\left.\frac{\partial p}{\partial \theta}\right|_{\substack{z=0\\ r\in X}} = 0\,. \tag{11}$$

From the above it is apparent that once we have adopted the assumption (5), the conditions (6) are a necessary supplement enabling that a homogeneous pressure field exists in the main plane, *i.e.* that we have

$$p = p(r, \theta)\,, \quad \text{when} \quad r \in X, \quad z = 0\,. \tag{12}$$

The last expression also yields Eqs (10) and (11). Expressions (5) may hold for the main plane only provided Eq. (12) is true, for a non-zero component of the pressure gradient would induce corresponding non-zero velocity gradient component.

*The Navier–Stokes equation for the coordinate r.* From Eqs (5) and (9) there follows that the Navier–Stokes equation for $z = 0$ and the axis $z$ takes the form

$$-g - \frac{1}{\varrho}\left.\frac{\partial p}{\partial z}\right|_{\substack{z=0\\ r\in X}} + \frac{\mu}{\varrho_f}\left.\frac{\partial^2 v_z}{\partial z^2}\right|_{\substack{z=0\\ r\in X}} + \left.\frac{\partial^2 v_z}{\partial r^2}\right|_{\substack{z=0\\ r\in X}} + \frac{1}{r}\left.\frac{\partial v_z}{\partial r}\right|_{\substack{z=0\\ r\in X}} = 0\,, \tag{13}$$

because as

$$\left.\frac{\partial^2 v_z}{\partial \theta^2}\right|_{\substack{z=0 \\ r\in X}} = 0 . \tag{14}$$

The orthogonal coordinates of the stress tensor in the main plane for $z = 0$ and $r \in X$ from Eqs (5), (8) and (9) are

$$\begin{aligned} p_{rr} &= p_{\theta\theta} = p_{zz} = -p , \\ \tau_{r\theta} &= \tau_{\theta r} = 0 , \\ \tau_{\theta z} &= \tau_{z\theta} = \mu \frac{\partial v_\theta}{\partial z} , \\ \tau_{rz} &= \tau_{zr} = \mu \left( \frac{\partial v_z}{\partial r} + \frac{\partial v_r}{\partial z} \right) . \end{aligned} \tag{15}$$

Subsequently one has to determine whether

$$\left.\frac{\partial v_\theta}{\partial z}\right|_{\substack{z=0 \\ r\in X}} \neq 0 , \quad \left.\frac{\partial v_r}{\partial z}\right|_{\substack{z=\theta \\ r\in X}} \neq 0 . \tag{15a}$$

Eq. (13) contains two dependent variables, $p = p(z)$ and $v_z = v_z(r, z)$. Hence, one needs at least one additional equation and boundary condition. If we put

$$p^* = p + g\varrho_f z \tag{15b}$$

then in view of Eq. (12) one may write Eq. (13) in the form

$$\mu \Delta \mathbf{v}\Big|_{\substack{z=0 \\ r\in X}} = \operatorname{grad} p^*\Big|_{\substack{z=0 \\ r\in X}} , \tag{16}$$

where $\Delta$ is the Laplace operator. If Eq. (16) holds then we have also

$$\mu \operatorname{div}(\Delta \mathbf{v})\Big|_{\substack{z=0 \\ r\in X}} = \operatorname{div}(\operatorname{grad} p^*)\Big|_{\substack{z=0 \\ r\in X}} \tag{17}$$

$$\mu \Delta(\operatorname{div} \mathbf{v})\Big|_{\substack{z=0 \\ r\in X}} = \Delta p^*\Big|_{\substack{z=0 \\ r\in X}} \tag{18}$$

$$\Delta p^*\Big|_{\substack{z=0 \\ r\in X}} = 0 \tag{19}$$

as the fluid is incompressible and hence div $v = 0$.

Eq. (*19*) is independent of Eq. (*13*) and represents the additional sought equation which, according to Eqs (*12*) and (*15*), in the cylindrical coordinates reads

$$\left.\frac{\partial^2 p}{\partial z^2}\right|_{\substack{z=0\\ r\in X}} = 0\,. \tag{20}$$

*The boundary conditions for Eqs (13) and (20).* According to the theoretical model the limiting case of the uniformly fluidized bed is an isolated particle falling at a terminal velocity $v_t$ in an unconfined quiescent fluid. This means that a solution of the mathematical model of the uniformly fluidized bed for $R \to \infty$ must reduce for the stream function, pressure and velocity components $v_r$, $v_0$, $v_z$ to the Stokes' solution in an unconfined fluid. Usually, expressions for these quantities in case of an isolated particle are expressed in terms of the spherical coordinates. After transformation into the cylindrical coordinates one obtains equations which may be used as necessary conditions for a test or the assessment of correctness of the expressions for the flow past a particle in the uniformly fluidized bed for $R = \infty$ and $z = 0$.

Stokes' solution in cylindrical coordinates is independent of $\Theta$ and reads

$$\psi(r, z)\big|_{R=\infty} = \frac{v_t r^2}{2}\left(1 - \frac{3r_0}{2(r^2 + z^2)^{1/2}} + \frac{r_0}{2(r^2 + z^2)^{3/2}}\right), \tag{21}$$

$$v_r(r, z)\big|_{R=\infty} = -\frac{3v_t r_0 rz}{4(r^2 + z^2)^{3/2}} + \frac{3v_t r_0^3 rz}{4(r^2 + z^2)^{5/2}} = -\frac{1}{r}\frac{\partial\psi}{\partial z}\,, \tag{22}$$

$$v_\theta(r, z)\big|_{R=\infty} = 0 \tag{23}$$

$$v_z(r, z)\big|_{R=\infty} = -\frac{3r_0 v_t z^2}{4}\left[\frac{1}{(r^2 + z^2)^{3/2}} - \frac{r_0^2}{(r^2 + z^2)^{5/2}}\right] - \\ - \frac{3r_0 v_t}{4(r^2 + z^2)^{1/2}} - \frac{r_0^3 v_t}{4(r^2 + z^2)^{3/2}} + v_t\,, \tag{24}$$

or

$$v_z(r, z)\big|_{R=\infty} = \frac{3v_t r_0 r^2}{4}\left[\frac{1}{(r^2 + z^2)^{3/2}} - \frac{r_0^2}{(r^2 + z^2)^{5/2}}\right] + \\ + v_t\left[1 - \frac{3r_0}{2(r^2 + z^2)^{1/2}} + \frac{r_0^3}{2(r^2 + z^2)^{3/2}}\right] = \frac{1}{r}\frac{\partial\psi}{\partial r}\,, \tag{25}$$

$$p\big|_{R=\infty} = p\infty - \frac{3\mu v_t r_0 z}{2(r^2 + z^2)^{3/2}}\,. \tag{26}$$

Additional suplementary conditions to Eqs (*13*) and (*20*) shall be derived by the following argument: Consider a ring of fluid symmetrically on both sides of the main plane in cylindrical coordinates for $r \in (r_0, R)$ as in Fig. 2. This Fig. shows a cut ABCD through the particle's center at $\theta = \text{const.}$ by a plane perpendicular to the main plane. The shape of this cut is independent of the angle $\theta$. Let $\boldsymbol{p}_z$, or $\boldsymbol{p}_r$, be the stress vector at the point $M(r, \theta, 0)$ in the elementary surface perpendicular to $z$, or $r$. A projection of the vector $\boldsymbol{p}_z$, or $\boldsymbol{p}_r$, into the direction of the axis $z$ shall be designated as $p_{zz}$ or $\tau_{zr}$. If from the volume forces only the gravity acts on the fluid then, using Fig. 2, we may write

$$-g\varrho_f[\pi(r+\mathrm{d}r)^2 - \pi r^2]\,\mathrm{d}z + 2\pi(r+\mathrm{d}r)\left(\tau_{zr} + \frac{1}{2}\frac{\partial \tau_{zr}}{\partial r}\mathrm{d}r\right)\mathrm{d}z - $$

$$- 2\pi r\left(\tau_{zr} - \frac{1}{2}\frac{\partial \tau_{zr}}{\partial r}\mathrm{d}r\right)\mathrm{d}z + [\pi(r+\mathrm{d}r)^2 - \pi r^2]\,.$$

$$\cdot\left[p_{zz} + \frac{1}{2}\frac{\partial p_{zz}}{\partial z}\mathrm{d}z - \left(p_{zz} - \frac{1}{2}\frac{\partial p_{zz}}{\partial z}\mathrm{d}z\right)\right] = 0\,. \qquad (27)$$

Eq. (*27*) rearranged and after neglecting small first-order quantities yields

$$-g\varrho_f + \frac{\partial \tau_{zr}}{\partial r} + \frac{1}{r}\tau_{zr} + \frac{\partial p_{zz}}{\partial z} = 0\,. \qquad (28)$$

After substitution from Eq. (*15*) into (*28*) we obtain

$$-g\varrho_f - \left.\frac{\partial p}{\partial z}\right|_{\substack{z=0\\ r\in X}} + \mu\left(2\left.\frac{\partial^2 v_z}{\partial z^2}\right|_{\substack{z=0\\ r\in X}} + \left.\frac{\partial^2 v_z}{\partial r^2}\right|_{\substack{z=0\\ r\in X}} + \left.\frac{\partial^2 v_r}{\partial r\,\partial z}\right|_{\substack{z=0\\ r\in X}} + \right. \qquad (29)$$

$$\left. + \frac{1}{r}\left.\frac{\partial v_z}{\partial r}\right|_{\substack{z=0\\ r\in X}} + \frac{1}{r}\left.\frac{\partial v_r}{\partial z}\right|_{\substack{z=0\\ r\in X}}\right) = 0\,,$$

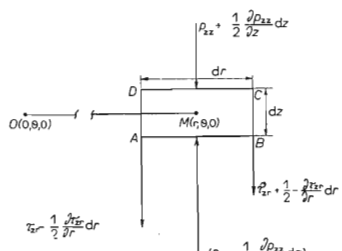


FIG. 2
Stresses Assigned to Surfaces on an Infinitesimal Ring of Fluid in Cylindrical Coordinates

for we generally have

$$p_{zz} = -p + 2\mu \frac{\partial v_z}{\partial z}, \quad \text{or} \quad \frac{\partial p_{zz}}{\partial z} = -\frac{\partial p}{\partial z} + 2\mu \frac{\partial^2 v_z}{\partial^2 z}. \tag{30}$$

A comparison of Eq. (*13*) and (*29*) yields the relation

$$\left.\frac{\partial^2 v_z}{\partial z^2}\right|_{\substack{z=0\\ re X}} + \frac{1}{r}\left.\frac{\partial v_r}{\partial z}\right|_{\substack{z=0\\ re X}} + \left.\frac{\partial^2 v_r}{\partial r\, \partial z}\right|_{\substack{z=0\\ re X}} = 0. \tag{31}$$

Eqs (*13*) and (*31*) are met provided we substitute from Eqs (*22*) through Eq (*26*), which is a necessary condition for their adequacy.

Eq. (*31*) yields important boundary conditions

$$\left.\frac{\partial v_r}{\partial z}\right|_{\substack{z=0\\ re X}} = 0, \quad \left.\frac{\partial^2 v_r}{\partial r\, \partial z}\right|_{\substack{z=0\\ re X}} = 0, \tag{32}$$

$$\left.\frac{\partial^2 v_z}{\partial z^2}\right|_{\substack{z=0\\ re X}} = 0, \tag{33}$$

$$\left.\frac{\partial^2 v_z}{\partial z^2}\right|_{\substack{z=0\\ r=r_0\\ R>r_0}} = \frac{1}{r_0}\left.\frac{\partial v_z}{\partial r}\right|_{\substack{z=0\\ r=r_0\\ R>r_0}}, \tag{34}$$

$$\left.\frac{\partial^2 v_z}{\partial r^2}\right|_{\substack{z=0\\ r=R}} = \frac{g\varrho_f}{\mu} + \frac{1}{\mu}\left.\frac{\partial p}{\partial z}\right|_{\substack{z=0\\ r=R}} \tag{35}$$

and other expression which may be useful in the solution of the problem of the flow past a particle within the bed.

These other conditions and relations are obtained by the following arguing: Let us designate a set of streamlines passing in the main plane through the circle of radius $r \in (r_0, R)$ with the center coinciding with that of the particle, by the term adjoined and the enveloped surface formed by these streamlines is the surface of adjoined streamlines. For a given $r$ each particle is assigned equal surface of adjoined streamlines. The planes parallel to the main plane intersect with the surface of adjoined streamlines in closed curves. According to the geometrical configur ation of particles in the structures of type A and B these closed curves deviate from the circle the less the greater the porosity and the smaller the distance of the given plane from the main plane. For an isolated particle in an unconfined fluid $\varepsilon \to 1$, these curves become circles in an arbitrary vertical distance from the main plane and an arbitrary $r$.

If in the cylindrical coordinates according to Fig. 1 one draws through the origin a plane $\theta$ = const. (perpendicular to the main plane) its intersections with the surfaces

of adjoined streamlines form streamlines falling into this plane. Corresponding images of the streamlines shall be termed lines $n$. A set of $n$ lines for an arbitrary $r$ is, for the structures $A_1$, $A_2$, $A_x$ and $B_1$, symmetric with respect to the axis $z$ passing through the center of the particle but the shape of the $n$ lines for a given $r$ depends on the angle $\theta$ and repeats after a certain period of values $\theta$. In case of structure $B_2$ and $B_3$ this symmetry remains preserved only for certain angles $\theta$. In case of the flow past an isolated particle in an uncofined fluid, $\theta$ has no effect on the shape of the $n$ lines characterized in Fig. 3. The $m$ lines are perpendicular to the $n$ lines and each of them is the line of constant potential of the velocity vector which is the potential vector. The line $m = 0$ falls into the main plane.

A family of the surfaces of the adjoined streamlines continuously fills the space assigned to the flow past the particle, excepting the normal passing through particle's center. The family of the $n$ lines fills continuously the plane $\theta = \text{const.}$ in the region corresponding to the flow of fluid passing past the particle. The velocity vector $\boldsymbol{v}$ in an arbitrary point $M(r, \theta = \text{const.}, z)$ is thus situated as a tangent to the line $n$ passing through this point. This vector makes with the vertical an angle $\beta$ which shall be taken positive if the velocity component $v_r$ is oriented toward the origin of the coordinates. Thus we may write

$$v_z = v \cos \beta , \qquad (36)$$

$$v_r = -v \sin \beta$$

and also

$$v_r = -v_z \operatorname{tg} \beta . \qquad (37)$$

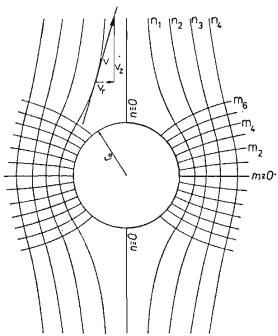


FIG. 3

Streamline (lines $n_1, n_2, \ldots$) and Equipotential Line (lines $m_1, m_2, \ldots$) for Flow Pattern under the Creeping Flow Past an Isolated Particle in an Unconfined Fluid

From the last equation we have

$$\frac{\partial v_r}{\partial z} = -\frac{\partial v_z}{\partial z}\operatorname{tg}\beta - v_z\frac{\partial \operatorname{tg}\beta}{\partial z}, \tag{38}$$

For $z = 0$ Eq. (9) holds and thus

$$\left.\frac{\partial v_r}{\partial z}\right|_{\substack{z=0\\ r\in X}} = -\left(v_z\frac{\partial \beta}{\partial z}\right)\Big|_{\substack{z=0\\ r\in X}}, \tag{39}$$

because for $z = 0$ beta equals zero and hence

$$\frac{\partial \operatorname{tg}\beta}{\partial z} = \frac{\partial \operatorname{tg}\beta}{\partial \beta}\frac{\partial \beta}{\partial z} = \frac{1}{\cos^2\beta}\frac{\partial \beta}{\partial z}. \tag{40}$$

In analogous manner we obtain from Eqs (37) and (38)

$$\left.\frac{\partial^2 v_r}{\partial r\,\partial z}\right|_{\substack{z=0\\ r\in X}} = -\left.\frac{\partial v_z}{\partial r}\right|_{\substack{z=0\\ r\in X}}\left.\frac{\partial \beta}{\partial z}\right|_{\substack{z=0\\ r\in X}} - \left[v_z\frac{\partial}{\partial r}\left(\frac{\partial \beta}{\partial z}\right)\right]\Big|_{\substack{z=0\\ r\in X}} = -\frac{\partial}{\partial r}\left(v_z\frac{\partial \beta}{\partial z}\right)\Big|_{\substack{z=0\\ r\in X}}. \tag{41}$$

An arbitrary plane $\theta = \text{const.}$ passing through the center of the particle perpendicularly to the main plane is an osculating plane for all encompassed streamlines at the points where these intersect the main plane. If $\varrho$ is the radius of curvature of the streamline for $z = 0$ then its corresponding $n$ line in the close vicinity of the main plane may be identified with the circle of radius equal to the radius of curvature $\varrho$. According to Fig. 4 where $\Delta n'$ is the length of arc on the circle of radius $\varrho$ corresponding to the angle $\beta'$ we may write

$$\beta = \Delta n'/\varrho = \arcsin\left(\Delta z/\varrho\right),$$

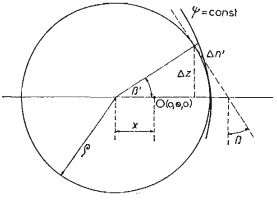


FIG. 4

Sketch of the Radius of Curvature of the Streamlines in the Main Plane under the Creeping Flow

because $\beta = \beta'$. From this

$$\left.\frac{\partial\beta}{\partial z}\right|_{\substack{z=0\\ r\in X}} = \lim_{\Delta z\to 0}\left[\frac{1}{\sqrt{\left(1-\frac{(\Delta z)^2}{\varrho^2}\right)}}\left(\frac{1}{\varrho}-\frac{\Delta z}{\varrho^2}\frac{\partial\varrho}{\partial z}\right)\right]_{\substack{z=0\\ r\in X}} = \frac{1}{\varrho}. \tag{42}$$

The values of $\varrho$ are known for two limiting conditions: *a*) According to the theoretical model for the creeping flow past the particle we have

$$\varrho \to r_0\,, \quad \text{when} \quad z = 0 \quad \text{and} \quad r \to r_0\,, \quad \varepsilon \in \langle \varepsilon_{\min}, 1\rangle\,. \tag{43}$$

*b*) For $R \to \infty$, or $\varepsilon \to 1$ (isolated particle in an unconfined fluid) we have

$$\varrho = (4r^4 - 3r_0r^3 - r_0^3r)/3r_0(r^2 - r_0^2) \tag{44}$$

or

$$\varrho^+ = \varrho/r_0 = (4r^{+4} - 3r^{+3} - r^+)/3(r^{+2} - 1)\,, \tag{45}$$

where $r^+ = r/r_0$. Eqs (*44*) and (*45*) are equivalent.

The derivation of Eq. (*45*): Eq. (*45*) has been derived from (*21*) after its arrangement to the form

$$\psi(r, z)|_{R=\infty} = \frac{v_1 r_0^2}{2}\left(\frac{r}{r_0}\right)^2\{1 - 3/2[(r/r_0)^2 + (z/r_0)^2]^{1/2} + 1/2[(r/r_0)^2 + (z/r_0)^2]^{3/2}\}\,. \tag{46}$$

Putting, in Eq. (*46*) $\psi(r, z)|_{R=\infty} = \text{const.} = \psi_i$, where $\psi_i \in \langle 0, \infty\rangle$ we obtain an equation for the streamline in dimensionless variables $z/r_0$ and $r/r_0$ which, for $z = 0$ intersects perpendicularly the main plane. From Fig. 3 it is apparent that the independent variable of the implicit function is $z/r_0$ because a single value $r/r_0$ has two values $z/r_0$. If Fig. 3 is rotated so that the positive direction of the axis $r$ in the cylindrical coordinates becomes identical with the positive direction of axis $r/r_0$ then the positive direction of the ordinates becomes identical with the negative direction of the axis $z$ and for the independent variable in the expression for the stream line one has to take

$$x = -z/r_0\,. \tag{47}$$

Then the dependent variable is

$$y = r/r_0\,. \tag{48}$$

The streamlines for $r/r_0 < 1$ are curves oriented in the direction of the negative

axis $z$. Positive normal to the streamline for $z = 0$ is directed as the positive axis $r/r_0$ and the center of curvature falls onto the negative normal. This means that the curvature of the streamline is negative and the computed radius of curvature $\xi$ has a sign opposite to that of the quantity $\varrho$ in Eq. (*44*).

Let us rewrite Eq. (*46*) in an implicit form

$$F(x, y) \equiv \frac{v_t r_0^2}{2} y^2 \{1 - 3/2[y^2 + (-x)^2]^{1/2} + 1/2[y^2 + (-x)^2]^{3/2}\} - \psi_i = 0 , \tag{49}$$

where $\psi_i$ is a constant. Then we have

$$\varrho^+ = -\xi/r_0 = (F_x'^2 + F_y'^2)^{3/2} / \begin{vmatrix} F''_{xx}, F''_{xy}, F'_x \\ F''_{yx}, F''_{yy}, F'_y \\ F'_x, F'_y, 0 \end{vmatrix} . \tag{50}$$

The symbols $F'$ or $F''$ designate the first and second order partial derivatives of the function $F(x, y)$ with respect to the variables shown by the subscript. For $z = 0$ we may write

$$-\varrho^+ = \zeta/r_0 = -F'_y(0, y)/F''_{xx}(0, y) = -(4y^4 - 3y^3 - y)/3(y^2 - 1) . \tag{51}$$

According to Eq. (*48*), we can infer that Eqs (*45*) and (*51*) are identical.

Equation (*42*) plays an important role in the formulation of the boundary conditions for Eqs (*13*) and (*20*). After substitution into Eq. (*31*) from Eqs (*39*), (*41*) and (*42*) we obtain

$$\left.\frac{\partial^2 v_z}{\partial z^2}\right|_{\substack{z=0 \\ r\in X}} - \left.\frac{v_z}{r\varrho}\right|_{\substack{z=0 \\ r\in X}} - \left.\frac{1}{\varrho}\frac{\partial v_z}{\partial r}\right|_{\substack{z=0 \\ r\in X}} - \left[v_z \frac{\partial}{\partial r}\left(\frac{1}{\varrho}\right)\right]_{\substack{z=0 \\ r\in X}} = 0 , \tag{52}$$

or

$$\left.\frac{\partial^2 v_z}{\partial z^2}\right|_{\substack{z=0 \\ r\in X}} - \frac{1}{r}\frac{\partial}{\partial r}\left(\frac{r v_z}{\varrho}\right)_{\substack{z=0 \\ r\in X}} = 0 . \tag{53}$$

In the points of contact of the two boundary circles we must have according to the theoretical model that

$$\left.\frac{\partial \beta}{\partial z}\right|_{\substack{z=0 \\ r=R}} = \frac{1}{\varrho} = 0 \tag{54}$$

because the vertical plane passing through the contact point of the two boundary circles separates equal subspaces of the stream around two neighbouring particles.

Corresponding streamlines on a finite segment on both sides of the main plane shall be perpendicular to this plane.

Owing to the continuous distribution of the velocity vector the streamlines passing through the remaining points of the boundary circle satisfy condition (*51*) but the section where these remain perpendicular diminishes with increasing distance from the point of contact of the boundary circles.

For the boundary circle thus we have generally

$$1/\varrho \to 0\,, \quad \text{when} \quad r \to R\,, \quad z = 0\,. \tag{55}$$

If for the boundary circle Eq. (*55*) is valid, then owing to the continuous change of the velocity vector we may write for the region of constant velocity between two boundary circles that

$$1/\varrho = 0\,, \quad \text{when} \quad r > R\,, \quad z = 0\,. \tag{56}$$

From Eqs (*55*) and (*56*) there follows

$$1/\varrho = 0\,, \quad \text{when} \quad r \geqq R\,, \quad z = 0\,. \tag{57}$$

From Eqs (*57*), (*49*) and (*39*), or from Eqs (*41*), we get $(32)_1$ or $(32)_2$. From Eqs (*31*), $(32)_1$ and $(32)_2$ we have in turn Eq. (*33*).

For the creeping flow past the particle we have $\varrho \to r_0$ if $r \to r_0$ for $z = 0$, $R > r_0$. From Eq. (*42*) then follows

$$\left.\frac{\partial \beta}{\partial z}\right|_{\substack{z=0\\ r=r_0\\ R>r_0}} = \frac{1}{r_0}\,, \quad \text{or} \quad \left.\varrho\right|_{\substack{z=0\\ r=r_0\\ R>r_0}} = r_0\,. \tag{58}$$

Since the fluid with internal friction satisfies

$$v_z(r_0, \theta, 0) = 0\,, \tag{59}$$

one obtains from Eq. (*58*) and (*39*) or (*41*) that

$$\left.\frac{\partial v_r}{\partial z}\right|_{\substack{z=0\\ r=r_0\\ R>r_0}} = 0 \quad \text{or} \quad \left.\frac{\partial^2 v_r}{\partial r\, \partial z}\right|_{\substack{z=0\\ r=r_0\\ R>r_0}} = -\frac{1}{r_0}\left.\frac{\partial v_z}{\partial r}\right|_{\substack{z=0\\ r=r_0\\ R>r_0}}. \tag{60}$$

From Eqs (*31*) and (*60*) there follows Eq. (*34*).

The function $v = v_z(r, \theta, 0)$ on the connecting line of the centers of two neighbouring particles passing through the point of contact of the two adjacent boundary

circles may take formally the form according to Fig. 5 or 6. For a fluid with internal friction the situation is as that in Fig. 5 according to which

$$\left.\frac{\partial v_z}{\partial r}\right|_{\substack{z=0\\ r \geq R}} = 0\,, \tag{61}$$

The validity of Eq. (61) for $r > R$ follows from the theoretical model because in region with constant velocity between the boundary circles is

$$v_z\Big|_{\substack{z=0\\ r>R}} = u = \text{const.} \tag{62}$$

From Eqs (61), (33) and (13) we get Eq. (35). In case of an isolated particle when $\varepsilon = 1$ or $R = \infty$ then

$$\left.\frac{\partial p}{\partial z}\right|_{\substack{z=0\\ r=\infty}} = \left.\frac{\partial p_\infty}{\partial z}\right|_{\substack{z=0\\ r=\infty}} = -g\varrho_f\,. \tag{63}$$

From Eqs (35) and (63) there follows

$$\left.\frac{\partial^2 v_z}{\partial r^2}\right|_{\substack{z=0\\ r=R=\infty}} = 0\,. \tag{64}$$

Analysis of the left hand side of Eq. (35) requires following considerations regarding the value of $\partial p/\partial z$. From the force balance and Eq. (12) there follows that between

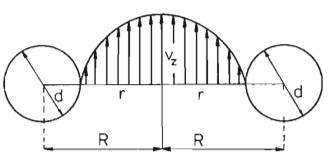


FIG. 5

Assumed Velocity Profile in the Main Plane on Line Connecting Centers of two Neighbouring Particles Passing through the Point of Contact of the Boundary Circles Assigned to these Particles

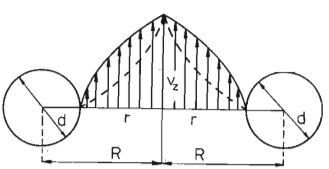


FIG. 6

Formally Possible but in a Real Fluid Improbable Velocity Profile in the Main Plane on the Line as on the Previous Figure

two main planes in an arbitrary stream tube the decrease of the static head amounts to

$$[-g\varrho_f - g(\varrho_s - \varrho_f)(1 - \varepsilon)]\, h = \int_0^h \frac{\partial p}{\partial z}\, dz\,. \tag{65}$$

For local values under the creeping flow past the particle we have

$$\partial p/\partial z = \partial p_1/\partial z + \partial p_2/\partial z + \partial p_3/\partial z\,, \tag{66}$$

where $\partial p_1/\partial z$ characterizes expansion or contraction of the stream tube; $\partial p_2/\partial z$ corresponds to the increase of potential energy of the fluid, and $\partial p_3/\partial z$ is a measure of dissipation of the mechanical energy due to the viscous friction. According to the theoretical model the cross section in each or in every second main plane is the same and hence

$$\int_0^h \frac{\partial p_1}{\partial z}\, dz = 0 \quad \text{or} \quad \int_0^{2h} \frac{\partial p_1}{\partial z}\, dz = 0\,. \tag{67}$$

We have also clearly

$$\int_0^h \frac{\partial p_2}{\partial z}\, dz = -g\varrho_f h\,, \quad \partial p_2/\partial z = -g\varrho_f\,. \tag{68}$$

From Eqs (66) through (68) we obtain

$$\int_0^h \frac{\partial p_3}{\partial z}\, dz = -g(\varrho_s - \varrho_f)(1 - \varepsilon)\, h \tag{69}$$

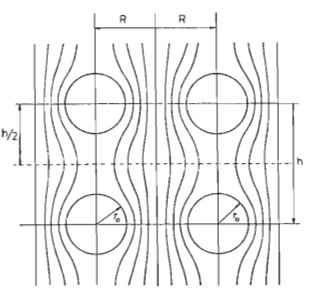


FIG. 7

Streamline Pattern for Structures $A_1$, $A_2$, $A_3$ in the Vertical Plane Passing in the Main Plane through the Particle Centers and Points of Contact of Boundary Circles

or

$$\int_0^{2h} \frac{\partial p_3}{\partial z} \, \mathrm{d}z = -2g(\varrho_s - \varrho_f)(1 - \varepsilon) h \,. \tag{70}$$

Since according to Eqs (9) and (61) the elementary stream tubes passing through the boundary circle within an infinitesimal neighbourhood of the main plane do not change its cross sectional area we have

$$\left.\frac{\partial p_1}{\partial z}\right|_{\substack{z=0 \\ r \geq R}} = 0 \,. \tag{71}$$

Fig. 7 depicts the streamline for any of the structures A, $A_2$, $A_x$ in the plane $\theta =$ = const. passing through the points of contact of the boundary circles. The shape of the streamlines is symmetrical with respect to the horizontal plane in the middle between two adjacent main planes. This symmetry of the flow past the particle remains preserved in any arbitrary vertical plane passing through the particle center. A more complex picture of the streamline pattern appears during the flow past a particle in the structure $B_2$ or $B_3$. Fig. 8 gives the expected pattern of the streamlines in case of the structure $B_2$ in the plane $\theta$ = const., whose contour is shown in Fig. 11 by a straight line. The symmetry of the streamlines exists only with respect to the main planes.

According to Fig. 7 it must be expected that between two main planes the values of $p_3$ for an elementary stream tube which envelopes an arbitrary streamline

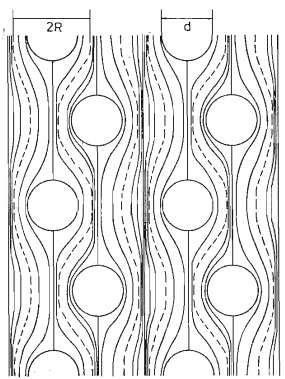


FIG. 8

Streamline Pattern for Structure $B_2$ in one of the Vertical Planes Passing in the Main Plane through Particle Centers

gradually depart symmetrically on both sides from the straight line

$$Y = p_0 - g(\varrho_s - \varrho_f)(1 - \varepsilon) h , \tag{72}$$

where $p_0$ is the static pressure on the given main plane from which the values of $h$ are calculated. For the stream tubes passing through the boundary circle we adopt, appart from Eq. (*72*), and additional assumption in the form

$$\left.\frac{\partial p_3}{\partial z}\right|_{\substack{z=0\\r=R}} = -g(\varrho_s - \varrho_f)(1 - \varepsilon) . \tag{73}$$

The assumption (*73*) expresses the fact that, apart from the mentioned symmetry, Eq. (*71*), holds and the streamlines passing through the boundary circle remain perpendicular to the main plane in a finite distance, *i.e.* there is no bending or expansion of the streamtubes which could cause deviations of the expression on the left hand side of Eq. (*73*) from the mean value given by the right hand side of (*73*).

The streamlines in Fig. 8 passing through the boundary circle are shown by broken lines. As these are symmetric with respect to any main plane, *i.e.* that Eq. (*71*) is valid, and remain perpendicular within a finite distance from the main plane, one has to expect even in this case the validity of Eq. (*73*).

According to Eqs (*66*), (*68*), (*71*) and (*73*) we have

$$\left.\frac{\partial p}{\partial z}\right|_{\substack{z=0\\r=R}} = -g\varrho_f - g(\varrho_s - \varrho_f)(1 - \varepsilon) . \tag{74}$$

On substituting from Eq. (*33*) and (*61*) into Eq. (*13*) we obtain (*35*). From Eq. (*35*) and (*74*) there follows

$$\left.\frac{\partial^2 v_z}{\partial r^2}\right|_{\substack{z=0\\r=R}} = -\frac{1}{\mu} g(\varrho_s - \varrho_f)(1 - \varepsilon) . \tag{75}$$

In accord with the above it is generally true that

$$\left.\frac{\partial p}{\partial z}\right|_{\substack{z=0\\reX}} = -g\varrho_f - g(\varrho_s - \varrho_f)(1 - \varepsilon) + \left.\frac{\partial P}{\partial z}\right|_{\substack{z=0\\reX}} , \tag{76}$$

where the expression $\left.\frac{\partial P}{\partial z}\right|_{\substack{z=0\\reX}}$ is, according to Eq. (*26*), a variable of some function

$$F\left(\left.\frac{\partial P}{\partial z}\right|_{\substack{z=0\\reX}}, \quad v_t, \mu, r_0, r, R\right) = 0 \tag{77}$$

from which it can be expressed explicitly. From Eq. (*74*) and (*76*) we have

$$\left.\frac{\partial P}{\partial z}\right|_{\substack{z=0\\ r\in X}} = 0 \,. \tag{78}$$

The validity of Eq. (*78*) for $r > R$ follows from the theoretical model because there are no velocity or pressure variations in region between the boundary circles. From Eqs (*13*), (*34*) and (*76*) we obtain after some arrangement

$$\left.\frac{\partial P}{\partial z}\right|_{\substack{z=0\\ r=r_0\\ R>r_0}} = g(\varrho_s - \varrho_f)\,(1-\varepsilon) = \mu\left[\left.\frac{\partial^2 v_z}{\partial r^2}\right|_{\substack{z=0\\ r=r_0\\ R>r_0}} + \frac{2}{r_0}\left.\frac{\partial v_z}{\partial r}\right|_{\substack{z=0\\ r=r_0\\ R>r_0}}\right]. \tag{79}$$

Since under the creeping flow past the particle there follows

$$v_t = \frac{2}{9}\,\frac{g r_0^2(\varrho_s - \varrho_f)}{\mu} \tag{80}$$

we may write

$$g(\varrho_s - \varrho_f) = \frac{9}{2}\,\frac{\mu v_t}{r_0^2} \tag{81}$$

or

$$\left.\frac{\partial P}{\partial z}\right|_{\substack{z=0\\ r=r_0\\ R>r_0}} = \frac{9}{2}\,\frac{\mu v_t}{r_0^2}(1-\varepsilon) + \mu\left[\left.\frac{\partial^2 v_z}{\partial r^2}\right|_{\substack{z=0\\ r=r_0\\ R>r_0}} + \frac{2}{r_0}\left.\frac{\partial v_z}{\partial r}\right|_{\substack{z=0\\ r=r_0\\ R>r_0}}\right], \tag{82}$$

Equations (*1*) through (*4*), (*13*), (*20*) and the boundary conditions represent the basic material for the mathematical solution of the flow past the particles in the main plane. The presence of the Laplace equations (*13*) or (*20*) in the set of equations is quite demanding as far as the boundary conditions are met. These requirements have not be thus far met.

In this work we shall show that with the above knowledge one can formulate a simplified mathematical model amenable to analytical method of solution. The results of the simplified solution enable formulation of the complex model.

*The Simplified Mathematical Model*

From the physical concept and Eq. (*54*) it is apparent that for porosities close to those at incipient fluidization the value of $\varrho$ causes to increase very rapidly with the distance

from particle's surface. According to Eq. (2) it means that in these cases the derivative

$$\left.\frac{\partial^2 v_z}{\partial z^2}\right|_{\substack{z=0\\ r\in X}}$$

vanishes very quickly. The quantity

$$\left.\frac{\partial^2 v_z}{\partial r^2}\right|_{\substack{z=0\\ r\in X}}$$

however, according to Eq. (75) retains large values of the order of magnitude $g(\varrho_s - \varrho_f)(1 - \varepsilon)$ in the whole interval $r \in \langle r_0, R\rangle$.

From this as well as from Eqs (13), (34) and (76) one can conclude that for porosities close to that of incipient fluidization we may write

$$\left.\frac{\partial p}{\partial z}\right|_{\substack{z=0\\ r\in X}} \ll \left.\frac{\partial^2 v_z}{\partial r^2}\right|_{\substack{z=0\\ r\in X}}, \quad \left.\frac{\partial p}{\partial z}\right|_{\substack{z=0\\ r\in X}} \ll g(\varrho_s - \varrho_f)(1 - \varepsilon), \tag{82a}$$

$$0\left(\left.\frac{\partial P}{\partial z}\right|_{\substack{z=0\\ r\in X}}\right) \doteq 0\left(\left.\frac{\partial^2 v_z}{\partial z^2}\right|_{\substack{z=0\\ r\in X}}\right). \tag{83}$$

From Eqs (13), (59), (61), (76), (82) and (83), after neglecting the terms $\left.\frac{\partial P}{\partial z}\right|_{\substack{z=0\\ r\in X}}$ and $\left.\frac{\partial^2 v_z}{\partial z^2}\right|_{\substack{z=0\\ r\in X}}$ there follows a simplified equation (13) with the boundary condition in the form

$$\frac{1}{r}\frac{\mathrm{d}}{\mathrm{d}r}\left(r\frac{\mathrm{d}v_z}{\mathrm{d}z}\right) = -K\,,$$

$$v_z(r_0, \theta, 0) = 0\,, \quad \left.\frac{\mathrm{d}v_z}{\mathrm{d}r}\right|_{r=R} = 0\,, \tag{84}$$

$$K = -g(\varrho_s - \varrho_f)(1 - \varepsilon)/\mu\,.$$

Eq. (84) together with Eqs (1) through (4) represent a simplified mathematical model of the flow past the particle in the main plane where for input quantities we take $w$, $d$, $\varepsilon$, $K$ (or Ar, Re, $\varepsilon$), $H_1$, $H_2\sigma(\varepsilon)$. According to the relationships defining $H_1$, $H_2$ and $\sigma$ one has to distinguish between three kinds of structural types 3

*a*) structural types $A_1$ and $B_1$, for which the corresponding quantities shall be designated by the superscript (1); *b*) structuraly types $A_2$, $B_2$ and $B_3$, for which the corresponding quantities shall be superscripted by (2); c) structural types $A_x$ distinguished by the superscript ($x$).

This means that for Eq. (*84*) there exist three different groups or relations for $H_1$, $H_2$ and $\sigma$; thus we have three simplified mathematical models. Only one of these though represents the uniformly fluidized bed in the state close to incipient fluidization. Solution of this model with the aid of the experimental data for Ar, Re and $\varepsilon$ for the expansion of the uniformly fluidized bed enables the value of $h/R = \varphi(\varepsilon)$ to be determined. The computed value of $h/R$ at the porosity of incipient fluidization $\varepsilon_{min} \in \langle 0{\cdot}412; 0{\cdot}420 \rangle$ must be identical, within experimental error, with the value tabulated in Table III of previous work[2] for the structural type characteristic for the uniformly fluidized bed. This identifies the geometrical configuration of particles in the uniformly fluidized bed in region close to incipient fluidization. The remaining two mathematical models cannot supply, for the values of Ar, Re and $\varepsilon$ measured during expansion of the uniformly fluidized bed, values of $h/R$ equal to those for incipient fluidization in Table III. This is so because individual structural types exhibit different characteristic triples of values Re, Ar and $\varepsilon$ than for the uniformly fluidized bed and the first condition of stability must be met[1].

*Solution of the Simplified Mathematical Model*

Eqs (*84*) yield the relations

$$v_z(r, 0, 0) = \frac{KR^2}{2} \ln \frac{2r}{d} - \frac{Kr^2}{4} + \frac{Kd^2}{16} \tag{85}$$

or

$$\int_{d/2}^{R} v_z r \, \mathrm{d}r = \frac{KR^4}{4} \ln \frac{2R}{d} - \frac{3KR^4}{16} + \frac{KR^2 d^2}{16} . \tag{86}$$

TABLE II

Parameters of the Uniformly Fluidized Bed for Structures $B_2$ or $B_3$ Based on Simplified Mathematical Model (Eqs (*96*), (*98*), (*103*), (*104*)) where $\varphi^{(2)}(\varepsilon) \equiv \varphi_*^{(2)}(\varepsilon)$ (from Table I)

| $\varepsilon$ | $u/v_t$ | $h/d$ | $l/d$ | $\varepsilon$ | $u/v_t$ | $h/d$ | $l/d$ |
|---|---|---|---|---|---|---|---|
| 0·400 | 0·0512 | 0·71252 | 1·1892 | 0·450 | 0·0779 | 0·71287 | 1·2418 |
| 0·408 | 0·0550 | 0·71266 | 1·1971 | 0·500 | 0·1129 | 0·71231 | 1·3029 |
| 0·412 | 0·05695 | 0·71270 | 1·2011 | 0·550 | 0·1580 | 0·71156 | 1·3742 |
| 0·416 | 0·0589 | 0·71276 | 1·2052 | 0·600 | 0·2145 | 0·71135 | 1·4577 |
| 0·420 | 0·0610 | 0·71282 | 1·2093 | 0·650 | 0·2841 | 0·71281 | 1·5567 |
| | | | | 0·700 | 0·3688 | 0·71737 | 1·6761 |

According to Eqs (*4*) and (*85*) we have

$$u = \frac{KR^2}{2} \ln \frac{2R}{d} - \frac{KR^2}{4} + \frac{Kd^2}{16} . \tag{87}$$

Solving Eqs (*1*), (*2*), (*86*) and (*87*) we obtain after rearrangement

$$\mathrm{Re}^{(i)} = w^{(i)} d \varrho_f / \mu = \tfrac{1}{18} \mathrm{Ar}\, \omega^{(i)}(\varepsilon) , \quad w^{(i)}/v_t = w^{(i)}(\varepsilon) , \tag{88}$$

There the superscript (i) = (1), (2), (x) refers to individual groups of structural types and we may write

$$\omega^{(1)}(\varepsilon) = 9(1-\varepsilon) \left\{ \left( \frac{\pi}{24(1-\varepsilon)\,\varphi^{(1)}(\varepsilon)} \right)^{2/3} \left( \ln \left[ 2 \left( \frac{\pi}{24(1-\varepsilon)\,\varphi^{(1)}(\varepsilon)} \right)^{1/3} \right] - \right. \right.$$

$$\left. \left. - \frac{8+\pi}{16} \right) + \frac{4+\pi}{32} - \frac{\pi}{256[\pi/24(1-\varepsilon)\,\varphi^{(1)}(\varepsilon)]^{2/3}} \right\} , \tag{89}$$

$$\omega^{(2)}(\varepsilon) = 9(1-\varepsilon) \left\{ \left( \frac{\pi}{12\sqrt{3}(1-\varepsilon)\,\varphi^{(2)}(\varepsilon)} \right)^{2/3} \left( \ln \left[ 2 \left( \frac{\pi}{12\sqrt{3}(1-\varepsilon)\,\varphi^{(2)}(\varepsilon)} \right)^{1/3} \right] - \right. \right.$$

$$\left. \left. - \frac{12+\pi\sqrt{3}}{24} \right) + \frac{6+\pi\sqrt{3}}{48} - \frac{\pi}{128\sqrt{3}[\pi/12\sqrt{3}(1-\varepsilon)\,\varphi^{(2)}(\varepsilon)]^{2/3}} \right\} , \tag{90}$$

$$\omega^{(x)}(\varepsilon) = 9(1-\varepsilon) \left\{ \left( \frac{\pi}{6\left(4 \operatorname{tg}\frac{\alpha}{2} + \frac{\sin 2\alpha}{\cos^2 \alpha/2}\right)(1-\varepsilon)\,\varphi^{(x)}(\varepsilon)} \right)^{2/3} \cdot \right.$$

$$\cdot \left( \ln \left[ 2 \left( \frac{\pi}{6\left(4 \operatorname{tg}\frac{\alpha}{2} + \frac{\sin 2\alpha}{\cos^2 \alpha/2}\right)(1-\varepsilon)\,\varphi^{(x)}(\varepsilon)} \right)^{1/3} \right] - \frac{1}{2} - \right.$$

$$- \frac{\pi}{4\left(4 \operatorname{tg}\frac{\alpha}{2} + \frac{\sin 2\alpha}{\cos^2 \alpha/2}\right)} \Bigg) + \frac{1}{8} + \frac{\pi}{8\left(4 \operatorname{tg}\frac{\alpha}{2} + \frac{\sin 2\alpha}{\cos^2 \alpha/2}\right)} -$$

$$\left. - \frac{4\pi}{256\left(4 \operatorname{tg}\frac{\alpha}{2} + \frac{\sin 2\alpha}{\cos^2 \alpha/2}\right)} \left[ \frac{\pi}{6\left(4 \operatorname{tg}\frac{\alpha}{2} + \frac{\sin 2\alpha}{\cos^2 \alpha/2}\right)(1-\varepsilon)\,\varphi^{(x)}(\varepsilon)} \right]^{-2/3} \right\} . \tag{91}$$

Eq. (85) can be rearranged using Eq. $(2)_3$ or the relationships for $R$ according to the Table I in ref.[2] to give

$$v_z^{(i)} d\varrho_f/\mu \equiv \mathrm{Re}_z^{(i)} = \tfrac{1}{18}\,\mathrm{Ar}\,\varkappa^{(i)}(\varepsilon)\,, \quad v_z^{(i)}/v_t = \varkappa^{(i)}(\varepsilon)\,, \quad (i) = (1), (2), (x)\,, \qquad (92)$$

where

$$\varkappa^{(1)}(\varepsilon) = 9(1-\varepsilon)\left\{[\pi/24(1-\varepsilon)\,\varphi^{(1)}(\varepsilon)]^{2/3}\ln 2r/d - r^2/2d^2 + 1/8\right\} \qquad (93)$$

$$\varkappa^{(2)}(\varepsilon) = 9(1-\varepsilon)\left\{[\pi/12\sqrt{3}(1-\varepsilon)\,\varphi^{(2)}(\varepsilon)]^{2/3}\ln 2r/d - r^2/2d^2 + 1/8\right\} \qquad (94)$$

$$\varkappa^{(x)}(\varepsilon) = 9(1-\varepsilon)\left\{\left[\frac{\pi}{6\left(4\,\mathrm{tg}\,\frac{\alpha}{2} + \frac{\sin 2\alpha}{\cos^2\alpha/2}\right)(1-\varepsilon)\,\varphi^{(x)}(\varepsilon)}\right]^{2/3}\ln\frac{2r}{d} - \frac{r^2}{2d^2} + \frac{1}{8}\right\}. \qquad (95)$$

In the region of constant velocity we have

$$\mathrm{Re}_u^{(i)} = u^{(i)}\,d\varrho_f/\mu = 1/18\;\mathrm{Ar}\,\xi^{(i)}(\varepsilon)\,, \quad \text{or} \quad u^{(i)}/v_t = \xi^{(i)}(\varepsilon)\,, \qquad (96)$$

There from Eq. (4) and (92) through (95) we have

$$\xi^{(1)}(\varepsilon) = 9(1-\varepsilon)\left\{[\pi/24(1-\varepsilon)\,\varphi^{(1)}(\varepsilon)]^{2/3}\left[\ln\left(2\,(\pi/24(1-\varepsilon)\,\varphi^{(1)}(\varepsilon)^{1/3}\right) - 1/2\right] + 1/8\right\}. \qquad (97)$$

$$\xi^{(2)}(\varepsilon) = 9(1-\varepsilon)\left\{[\pi/12\sqrt{3}(1-\varepsilon)\,\varphi^{(2)}(\varepsilon)]^{2/3}\left[\ln\left(2(\pi/12\sqrt{3}(1-\varepsilon)\,\varphi^{(2)}(\varepsilon)\right)^{1/3}\right) - 1/2\right] + 1/8\right\}, \qquad (98)$$

$$\xi^{(x)}(\varepsilon) = 9(1-\varepsilon)\left\{\left[\frac{\pi}{6\left(4\,\mathrm{tg}\,\frac{\alpha}{2} + \frac{\sin 2\alpha}{\cos^2\alpha/2}\right)(1-\varepsilon)\,\varphi^{(x)}(\varepsilon)}\right]^{2/3} \cdot \left[\ln\left(2\left(\frac{\pi}{6\left(4\,\mathrm{tg}\,\frac{\alpha}{2} + \frac{\sin 2\alpha}{\cos^2\alpha/2}\right)(1-\varepsilon)\,\varphi^{(x)}(\varepsilon)}\right)^{1/3}\right) - \frac{1}{2}\right] + \frac{1}{8}\right\}. \qquad (99)$$

Relationships (89) through (99) contain an unknown function $\varphi^{(i)}(\varepsilon) = (h/R)^{(i)}$ which must be found in a suitable manner.

*Calculation of* $h/R$. This calculation can be carried out from Eqs (88) through (90) by successive approximation. For this purpose we use the following equation

instead of Eq. (*88*)

$$\left|\omega_*^{(i)}(\varepsilon) - \frac{18\ \mathrm{Re}}{\mathrm{Ar}}\right| = \lambda\,. \qquad (100)$$

There $\lambda$ is small positive number. In the calculation we put $\lambda = 10^{-6}$ and $\lambda = 10^{-8}$. The values of $h/R$ calculated for these two cases differ only on the fifth decimal. The quantity Re in Eq. (*100*) does not have the superscript (i) ($i$ = 1, 2, x) for the values of Re are measured for the expansion of the uniformly fluidized bed whose structure is not known *a priori*. Expressions $\omega^{(i)}(\varepsilon)$ are defined formally in the same way as $\omega_*^{(i)}(\varepsilon)$ except that the former satisfy also the condition (*100*) which under the equality $\omega^{(i)}(\varepsilon) \equiv \omega_*^{(i)}(\varepsilon)$ holds only for the structural types corresponding to the uniformly fluidized bed Then the values $h/R = \varphi^{(i)}(\varepsilon)$ possess a physical meaning. The values $h/R$ for the remaining structural types are physically meaningless for the group Re/Ar measured in the uniformly fluidized bed does not correspond for given $\varepsilon$ to these structures.

For the uniformly fluidized bed at Ar $\leqq$ 7·2 we may write[6] with a relative error less than 5% the following Eq.

$$\mathrm{Re} = \tfrac{1}{18}\,\mathrm{Ar}\,\varepsilon^{4.65}\,. \qquad (101)$$

TABLE III

Data for the Assessment of Validity of Condition (*82*)

| $\varepsilon$ | $\frac{r_0^2}{v_t}\frac{\partial P}{\partial z}\Big\vert_{\substack{z=0\\r=r_0\\R>r}}$ | $-\frac{r_0^2}{v_t}\frac{\partial^2 v_z}{\partial r^2}\Big\vert_{\substack{z=0\\r=r_0\\R>r_0}}$ | $\frac{r_0^2}{\mu v_t}\,g(\varrho_s - \varrho_f)\,(1-\varepsilon)$ |
|---|---|---|---|
| 0·400 | 0·5592 | 3·2592 | 2·7 |
| 0·408 | 0·5769 | 3·2409 | 2·664 |
| 0·412 | 0·5857 | 3·2317 | 2·646 |
| 0·416 | 0·5945 | 3·2226 | 2·628 |
| 0·420 | 0·6034 | 3·2134 | 2·610 |
| 0·450 | 0·6709 | 3·1459 | 2·475 |
| 0·500 | 0·7848 | 3·0348 | 2·25 |
| 0·550 | 0·8995 | 2·9245 | 2·025 |
| 0·600 | 1·0123 | 2·8123 | 1·8 |
| 0·650 | 1·1209 | 2·6959 | 1·575 |
| 0·700 | 1·2213 | 2·5713 | 1·35 |

For the calculation of $h/R = \varphi(\varepsilon)$ we therefore may use the following equation instead of Eq. (*100*)

$$\left|\omega_*^{(i)}(\varepsilon) - \varepsilon^{4.65}\right| = \lambda\,. \qquad (102)$$

The values $h/R$ were calculated on the one hand from the experimental data given in ref.[6] from Eq. (*100*) and, on the other hand, from Eq. (*102*). Since the results did not differ appreciably, Table I provides only results following from Eq. (*102*). The quantities $\varphi_*^{(1)}(\varepsilon) = (h/R)^{(1)}$, or $\varphi_*^{(2)}(\varepsilon) = (h/R)^{(2)}$ have been assigned to the quantities $\omega_*^{(1)}(\varepsilon)$ or $\omega_*^{(2)}(\varepsilon)$. It can be shown that the values $\varphi_*^{(x)}(\varepsilon)$ computed from Eq. (*102*) for $\omega_*^{(x)}(\varepsilon)$ fall into the interval $(\varphi_*^{(1)}(\varepsilon),\ \varphi_*^{(2)}(\varepsilon))$ and vary with the magnitude of the angle $\alpha$.

From the above the value $\varphi_*^{(1)}(\varepsilon)$, $\varphi_*^{(2)}(\varepsilon)$ from Table I should be compared for $\varepsilon \in \langle 0{\cdot}412,\ 0{\cdot}420\rangle$ with the values $\varphi^{(i)}(\varepsilon) = h/R$ from Table III in ref.[2] which were derived from the geometrical concept for all plausible structural types. The content of the Table III from ref.[2] is shown graphically in Fig. 9. The uniformly fluidized bed at incipient fluidization exhibits that structure for which $\varphi_*^{(i)}(\varepsilon) = \varphi^{(i)}(\varepsilon)$. From this comparison it is clear that the uniformly fluidized bed at incipient fluidization can plausibly exhibit only structures $B_2$ or $B_3$. In addition the stratum of the fluidized state beginns by contact of particles from adjacent main planes while the particles within the main plane still do not contact each other. For this case the Table I shows values $h/R = \varphi(\varepsilon) = \varphi^{(2)}(\varepsilon)$ from Table III of ref.[2]. The agreement between $\varphi_*^{(2)}(\varepsilon)$ and $\varphi^{(2)}(\varepsilon)$ in Table I may be rated as very good. From Fig. 9 it is apparent that

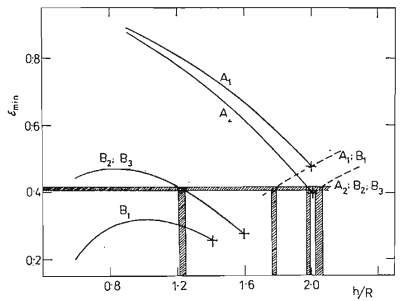


FIG. 9

Porosity $\varepsilon_{min}$ as a Function of $h/R = \varphi(\varepsilon)$ which May Cause in Beds of Various Structures the Loss of Fluidized State after Contact between Particles

$\varphi_*^{(1)}(\varepsilon)$ and $\varphi_*^{(x)}(\varepsilon)$ cannot belong in region of incipient fluidization to any structural type.

The geometrical configuration of particles in the main plane in the structure $B_2$ and $B_3$ is apparent from Fig. 10. Fig. 11 or Fig. 12 depict spatial configuration of the main planes in the structures $B_2$ or $B_3$.

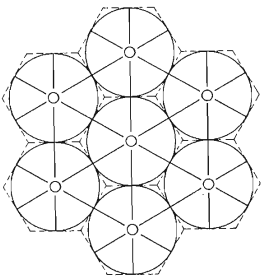

FIG. 10

Geometrical Configuration of Particles in the Main Plane for Structures $B_2$ and $B_3$

The circle within the hexagon is the boundary circle; internal circle depicts particle.

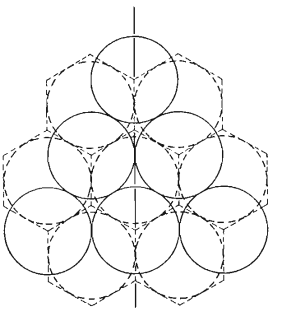

FIG. 11

Spatial Configuration of Main Planes in Structures $B_2$

Only boundary flow patterns with boundary circles are shown.

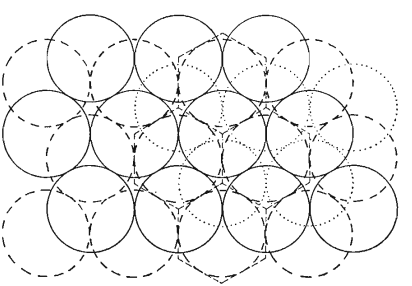

FIG. 12

Spatial Configuration of Main Planes in Structures $B_3$

Only boundary flow patterns and boundary circles are shown.

The geometrical configuration of particles in the structures of the type $B_2$ or $B_3$ significantly differs from that in the structures $A_1$, $A_2$, $A_x$ and $B_1$ (ref.[2]), which still strike the balance of the gravity, buoyancy and resistance forces for each particle. This justifies the assumption that the uniformly fluidized bed displays in the whole interval of porosity $\varepsilon \in \langle \varepsilon_{min}, 1 \rangle$ the structure of the type $B_2$ or $B_3$. The first condition of stability of the uniformly fluidized bed means that from all possible beds with the structures of the type A and B for given porosity $\varepsilon > \varepsilon_{min}$, superficial velocity of the fluid $W < w_{min}$, given particles and fluid, the uniformly fluidized will be the one minimizing the rate of mechanical energy dissipation in the course of the flow past the particles. The type of the structure must necessarily strongly influence the rate of dissipation for otherwise identical conditions and since the admissible structural types markedly differ, it is probable that the minimum rate of dissipation is associated with only one structural type.

Table II summarizes values $u/v_t$, $h/d$ and $l/d$ computed on the basis of the simplified mathematical model, assuming its validity up to the porosity 0·70 and the structures of the type $B_2$ or $B_3$. For the spacing $l$ of the centers of the particles in the main plane (see Fig. 10 of this paper and Table I in the previous paper[2]) we may write

$$l = 2R\,, \quad \text{or} \quad l = d = 2R/d = 2\left[(\pi/12\sqrt{3}(1-\varepsilon)\,\varphi^{(2)}(\varepsilon)\right])^{1/3}\,. \tag{103}$$

The quantity $h/d$ is given by

$$h/d = \left[(\pi/12\sqrt{3}(1-\varepsilon)\,\varphi^{(2)}(\varepsilon)\right]^{1/3}\varphi^{(2)}(\varepsilon)\,. \tag{104}$$

The values $l/d$, in accord with the theoretical considerations, satisfy the condition $l/d > 1$, *i.e.* no contact of particles in the main plane. The spacing of the main planes, measured by the dimensionless expression $h/d$, are smaller than in the case if in the structures $B_2$ and $B_3$ the particles should contact both between the adjacent main planes as well as with in the main plane. For this limiting case $\varepsilon_{min} = 0{\cdot}2595$, $h/d = 0{\cdot}8165$ and $h/l = d$.

Figs 13 through 15 show the velocity profiles in the main plane computed from Eqs (*92*) and (*94*) in terms of the dimensionless variables $v_z/v_t\big|_{\substack{z=0\\ r\leq R}}$ and $r/d$, for the structures $B_2$ and $B_3$. The values $\varphi^{(2)}(\varepsilon)$ for each $\varepsilon$ were computed in the same way as $\varphi_*^{(2)}(\varepsilon)$ in Table I. The broken line pertains to an isolated particle in an unconfined fluid when $R = \infty$.

From the approach applied in the process of the model simplification it follows that a solution of this model satisfies the conditions (*59*), (*61*), (*64*) and (*75*). For an arbitrary $R$ we may write

$$\left.\frac{\partial P}{\partial z}\right|_{\substack{z=0\\ r=r_0\\ R>r^0}} = \left.\frac{\partial^2 v_z}{\partial z^2}\right|_{\substack{z=0\\ r=r_0\\ R>r}}$$

*i.e.* condition (*83*) may be regarded as satisfied in view of Eqs (*53*) and (*78*). For large $R$, however, the conditions (*82*) are not met.

Table III summarizes data computed from the simplified model important for the assessment of validity of condition $(82)_1$. The values in the third and the fourth column of this table are the limiting values for the expression

$$-\frac{r_0^2}{\mu v_t} - \frac{\partial^2 v_z}{\partial r^2}\bigg|_{\substack{z=0 \\ R>r_0 \\ r\in X}} .$$




FIG. 13

Dimensionless Velocity Profile (approximation solution)

$v_z/v_t = F(r/d)$ for the flow past the particle in the uniformly fluidized bed with different porosity and for the creeping flow past an isolated particle. ——— particle within the bed, ----- isolated particle.

The quantity $\left.\frac{\partial P}{\partial z}\right|_{\substack{z=0\\r=r_0\\R>r_0}}$ for $\varepsilon = 0{\cdot}400$ is approximately six times smaller than $\left.\frac{\partial^2 v_z}{\partial r^2}\right|_{\substack{z=0\\r=r_0\\R>r_0}}$ but with increasing porosity both values converge. From Table III it may be assumed that Fig. 13 is a good approximation of reality. The curves in Figs 14 and 15 for $\varepsilon > 0{\cdot}8$ carry a large error.

LIST OF SYMBOLS

| | |
|---|---|
| A | structural type or cross sectional area of region of constant velocity within boundary flow pattern |
| $\mathrm{Ar} = gd^3(\varrho_s - \varrho_f)\,\varrho_f/\mu^2$ | Archimedes group |
| $d$ | diameter of spherical particle |
| $g$ | acceleration due to gravity |
| $F(x, y)$ | function in Eq. (*49*) |
| $F'_x$, $F'_y$ | first order partial derivatives of function $F(x, y)$ |
| $F''_{xx}$, $F''_{yy}$, $F''_{xy}$, $F''_{yx}$ | second order partial derivatives of $F(x, y)$ |
| $h$ | spacing of main planes |
| $H_1$ | coefficient from relation $S_1 = H_1 R^2$ from Table I of ref.[2] |
| $H_2$ | coefficient from $A = H_2 R^2$ from Table I of ref.[2] |
| (i) | superscript (1), (2), (x) distinguishing between three groups of simplified mathematical models describing three groups of structural types |
| $K$ | constant defined in Eq. $(84)_3$ |
| $l$ | spacing of center of particles in main plane, Eq. (*103*) |
| $m$ | equipotential lines (velocity as potential vector) |
| $n$ | pattern of stream lines on $\theta =$ const. plane passing through particle center as the origin of cylindrical coordinates |
| $P$ | pressure, Eq. (*76*) |
| $p$ | pressure in Navier–Stokes equations |
| $p^*$ | pressure, Eq. (*15a*) |
| $p_0$ | value of $p$ in main plane, as background pressure |
| $p_1, p_2, p_3$ | fictious components of pressure $p = p_1 + p_2 + p_3$ caused by expansion or contraction of streamtube ($p_1$), change of potential energy ($p_3$) and dissipation of mechanical energy ($p_3$) |
| $p_{rr}, p_{\theta\theta}, p_{zz}$ | normal components of stress tensor for a Newtonian fluid in cylindrical coordinates |
| $p_\infty$ | pressure in the plane of equator at $R = \infty$ for an isolated sphere where the relative motion of the fluid in an inertial frame of reference is caused only by the motion of the sphere |
| $r$ | radial cylindrical coordinate with the origin at the center of the particle, see Fig. 1 |
| $r^+$ | dimensionless cylindrical coordinate of radius $r^+ = r/r_0$ |
| $r_0$ | radius of spherical particle in the bed |
| R | radius of boundary circle |
| $\mathrm{Re} = \mathrm{d}w\,\varrho_f/\mu$ | Reynolds number |
| $\mathrm{Re}^{(i)} = \mathrm{d}w^{(i)}\,\varrho_f/\mu$ | Reynolds number (i) = (1), (2), (x) |
| $\mathrm{Re}_u^{(i)} = \mathrm{d}u^{(i)}\,\varrho_f/\mu$ | Reynolds number (i) = (1), (2), (x) |
| $\mathrm{Re}_z^{(i)} = \mathrm{d}v_z^{(i)}\,\varrho_f/\mu$ | Reynolds number (i) = (1), (2), (x) |

$S_1$ surface area of a boundary flow pattern

$u$ local velocity of fluid in the boundary circle and in region of constant velocity between boundary circles

$u^{(i)}$ value of $u$ for structural types (i) = (1), (2), (x))

$v_r$ radial velocity component in the boundary flow pattern in the principal plane

$v_t$ terminal velocity of settling of an isolated spherical particle in an unconfined real fluid

$v_z$ local $z$ component of velocity in main plane near the particle for $r < R$ (direction of axis $z$ in Fig. 1)

$v_\theta$ velocity component as in Fig. 1 in the boundary flow pattern

$w$ superficial velocity of fluid in the uniformly fluidized bed

$w^{(i)}$ superficial velocity for structures (i) = (1), (2), (x)

$w_{min}$ velocity at incipient fluidization

$x \equiv -z/r_0$

$X \equiv \langle r_0, R \rangle$

$y \equiv r/r_0$

$Y$ dependent variable, Eq. (*72*) with independent variable $h$

$z$ axial cylindrical coordinate, Fig. 1

$\alpha$ angle of as in Fig. 8 of ref.[1]

$\beta, \beta'$ angles as in Fig. 4

$\Delta n'$ length of arc on the circle of radius $\varrho$ for the angle $\beta'$, see Fig. 4

$\varepsilon$ porosity of uniformly fluidized bed

$\varepsilon_{min}$ porosity of uniformly fluidized bed at incipient fluidization, or minimum bed porosity

$\xi = -\varrho$

$\theta$ angular coordinate as in Fig. 1

$\varkappa^{(i)}(\varepsilon)$ function from Eq. (*92*), (i) = (1), (2), (X) given by Eqs (*93*)—(*95*) provided the fluid flows under the force balance on every particle

$\lambda$ constant in Eq. (*100*) or (*102*)

$\mu$ dynamic viscosity of fluid

$\nu$ kinematic viscosity of fluid

$\xi^{(i)}(\varepsilon)$ function in Eq. (*96*) for (i) = (1), (2), (x) given by Eqs (*97*)—(*99*)

$\varrho$ radius of curvature of streamline for $z = 0$, $r \in \langle r_0, R \rangle$

$\varrho^+ = \varrho/r_0$ dimensionless radius of curvature

$\varrho_f^{(\ )}$ fluid density

$\varrho_s$ particle density

$\sigma(\varepsilon)$ function from $R = d\sigma(\varepsilon)\,[\varphi(\varepsilon)]^{-1/3}$ for the uniformly fluidized bed

$\sigma^{(i)}(\varepsilon)$ function from $R^{(i)} = d\sigma^{(i)}(\varepsilon)\,[\varphi^{(i)}(\varepsilon)]^{-1/3}$ given in Table I of ref.[2] for (i) = = (1), (2), (x)

$\tau_{r\theta}, \tau_{\theta r}, \tau_{\theta z}, \varrho_{z\theta}, \tau_{rz}, \varrho_{zr}$ tangential components of stress tensor in cylindrical coordinates

$\varphi(\varepsilon) = h/R$ for uniformly fluidized bed

$\varphi^{(i)}(\varepsilon)$ ratio $h/R$ for structures (i) = (1), (2), (x) in case of force balance (gravity, buoyancy, resistance)

$\varphi_*^{(i)}(\varepsilon)$ computed from Eq. (*102*)

$\psi$ stream function

$\omega^{(i)}(\varepsilon)$ function from Eq. (*88*) for (i) = (1), (2), (x) given by Eqs (*89*)—(*91*)

$\omega_*^{(i)}(\varepsilon)$ function for (i) = (1), (2), (x) taking formally the same form as $\omega^{(i)}(\varepsilon)$ but nor necessarilly satisfying Eq. (*88*), which satisfies (*102*), *i.e.* the variable is $\varphi_*^{(i)}(\varepsilon)$

REFERENCES

1. Beña J.: This Journal *41*, 1976 (1976).
2. Beña J.: This Journal *41*, 1996 (1976).
3. McNown J. S.: Int. Congress Appl. Mech., Proc. p. 17, 7, II, 1948.
4. Hawksley P. G.: Symposium *Some Aspects of Fluid Flow*. Arnold, London 1950.
5. Richardson J. F., Zaki W. N.: Chem. Eng. Sci. *3*, 65 (1954).
6. Beña J., Ilavský J., Koszaczký E., Zákutný O.: Chem. Zvesti *13*, 170 (1959).

Translated by V. Staněk.